

# OBSERVING SIZE EFFECTS IN THE THERMAL BEHAVIOUR OF ROCKS

**A. Fehér**

*Department of Energy Engineering, Faculty of Mechanical Engineering,  
Budapest University of Technology and Economics  
Műegyetem rkp. 3., H-1111 Budapest – Hungary  
feher@energia.bme.hu*

**R. Kovács**

*Department of Energy Engineering, Faculty of Mechanical Engineering  
Budapest University of Technology and Economics  
Műegyetem rkp. 3., H-1111 Budapest – Hungary*

*Department of Theoretical Physics, Wigner Research Centre for Physics, Institute for  
Particle and Nuclear Physics, Budapest – Hungary*

## ABSTRACT

The classical constitutive equation for heat conduction, Fourier's law, plays an essential role in the engineering practise and holds only for homogeneous materials. However, most of the materials consist of certain sort of heterogeneity, such as porosity, cracks, or different materials are in contact.

We used heat pulse measurement method ("flash method"), a standard method in the engineering practise, to measure the thermal diffusivity of various rock samples. During the heat pulse experiment the pulse reaches the front of the sample, and the temperature of the rear is measured with a thermocouple and recorded. We found that the rear side temperature history can deviate from the one predicted by Fourier's law. Therefore, in the evaluation of the experimental data, we used an analytical solution of a non-Fourier model, called Guyer-Krumhansl equation. We present the measurement methodology and data recorded together with the evaluation procedure for two rock samples of types Szaszvar and Szarsomlyo Limestone formations from Hungary. We observed the size dependence of thermal diffusivity for both Fourier and non-Fourier models. Additionally, we also observed the size dependence of the non-Fourier effects, vanishing for thicker samples.

**Keywords:** heterogeneous materials, non-equilibrium thermodynamics, size effects, Guyer-Krumhansl equation

## INTRODUCTION

Engineering practice requires reliable methods to determine the necessary parameters that are sufficient to characterise the behaviour of a material. In the following, we focus on the thermal characterisation of materials, with particular emphasis on heterogeneous materials such as rocks. In previous publications [1, 2], it has been reported that the presence of different heterogeneities can lead to non-Fourier thermal conduction effects due to the simultaneous presence of thermal conduction channels with different characteristic times. Such effects can be observed in the so-called "flash" (heat pulse) experiment, in which the front face of the specimen is excited by a short thermal pulse and the temperature is measured on the rear side [3-5]. This temperature history is used to determine the thermal diffusivity to characterise the transient behaviour of the material.

This non-Fourier effect occurs over a specific time interval, as Figure 1 shows for a typical outcome of the flash experiments; this called over-diffusion. After that interval, the Fourier equation seems to be a suitable choice for modelling, the effect of heterogeneities disappears, furthermore there is no difference between the steady-states described by the Fourier and the non-Fourier heat equation, only the transient evolution of temperature differs in these cases. Our experimental experience suggests that the existence of over-diffusion depends on a number of factors, such as the sample thickness, the typical parallel time scales and the excitation (i.e., boundary conditions) [6].

The evaluation procedure for flash experiments with non-Fourier heat equations is not yet standard. Even numerically, finding solutions to non-Fourier models is not straightforward, some methods may lead to incorrect solutions [7], and commercial built-in algorithms are not efficient for these models.

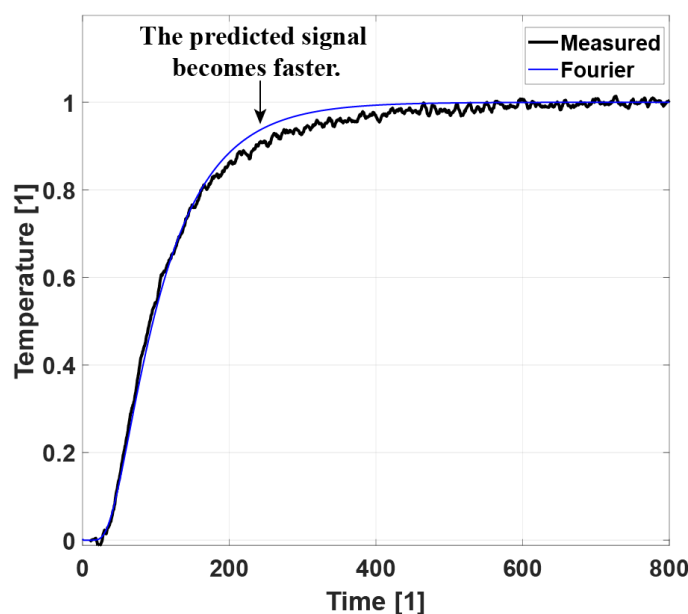


Fig. 1. Measured rear side temperature history for the rock sample and the prediction provided by Fourier's theory, where the dimensionless time is scaled by the heat pulse, which is 0.01 sec [8].

### Models for Heat Pulse Experiments

Although there are several generalisations of Fourier's law in the literature [9-14], there is only one of them that has been shown to be reasonable beyond Fourier theory, called the Guyer-Krumhansl (GK) equation [3]. The constitutive equation reads in one spatial dimension

$$\tau_q \partial_t q + q + \lambda \partial_x T - \kappa^2 \partial_{xx} q = 0. \quad (1)$$

In the equation,  $\tau_q$  is the relaxation time of the heat flux  $q$  and  $\kappa^2$  is a kind of 'dissipation parameter', usually related to the mean free path in kinetic theory. The  $\partial_{xx} q$  in the constitutive equation allows to properly characterise the so-called over-diffusive propagation, presented in Figure 1. When the equality  $\kappa^2/\tau_q = \alpha$  holds (with  $\alpha = \lambda/(\rho c)$ ), we call it Fourier resonance condition as that setting recovers the solutions of Fourier equation [2, 16]. Equation (1) is the time evolution equation for the heat flux, and to have a mathematically and physically complete system we need the balance of the internal energy  $e$ ,

$$\rho c \partial_t T + \partial_x q = 0, \quad (2)$$

in which the equation  $e = cT$  is used, where  $c$  is the specific heat and  $\rho$  is the mass density. All these coefficients are constant, we assume only rigid bodies without a volumetric heat source.

Fig. 2 shows the typical rear side solutions for the Fourier, Maxwell-Cattaneo-Vernotte (MCV) and GK models. It can be seen that while the MCV equation gives sharp wave fronts for the solution, the GK equation provides a significantly better character with the measured data, showing the observed thermal behaviour. Therefore, the GK equation appears to be a necessary extension of the Fourier equation that covers practical needs to determine the thermal properties of heterogeneous materials as accurately as possible.

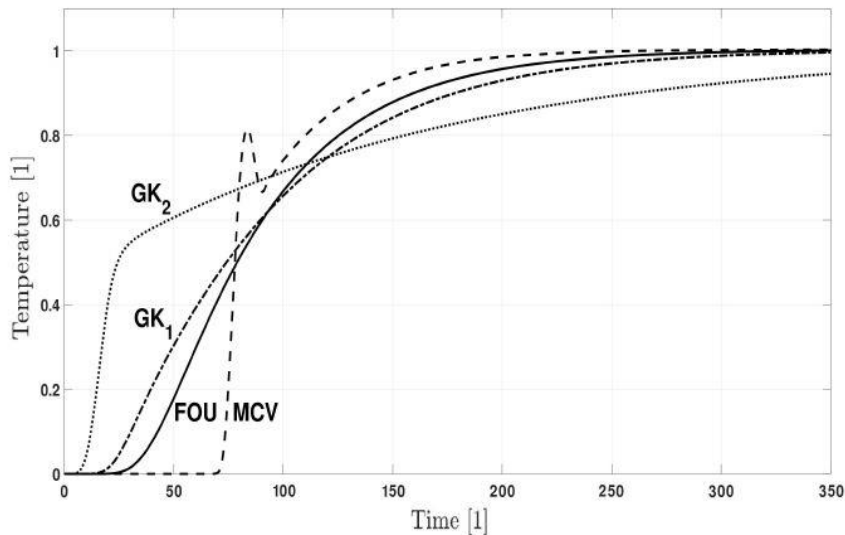


Fig. 2. Typical rear side temperature histories for the Fourier ("FOU"), Maxwell-Cattaneo-Vernotte ("MCV") and Guyer-Krumhansl ("GK1" and "GK2") equations. For the GK model, two different solutions are depicted here: "GK1" is a slightly over-diffusive one showing similar outcome with the experiments, while "GK2" is a strongly over-diffusive solution [8].

In the following, we briefly present the experimental settings together with the applied evaluation procedure for both Fourier and GK heat conduction equations. While for the Fourier equation the evaluation follows a standard, well-known methodology, the utilisation of the GK equation is not straightforward. Therefore, we shortly summarise the developed evaluation method based on [8] in Sec. 3. In Sec. 4., we present our new observations for Szaszvar and Szarsomlyo Limestone Formations in which we found size effects for both the thermal diffusivity and the over-diffusive non-Fourier effect.

## HEAT PULSE EXPERIMENT

The heat pulse experiments are used to measure the thermal diffusivity of a material by registering the rear side temperature history. For the specified settings, see Fig. 3 below. The front surface a sample is painted black for absorption, and the rear side is coated with silver in order to achieve good contact with the thermocouple. A flash lamp generates the heat pulse; its length is 0.01 seconds. For further details, we refer to the earlier papers published by our group, [1, 2, 6, 15].

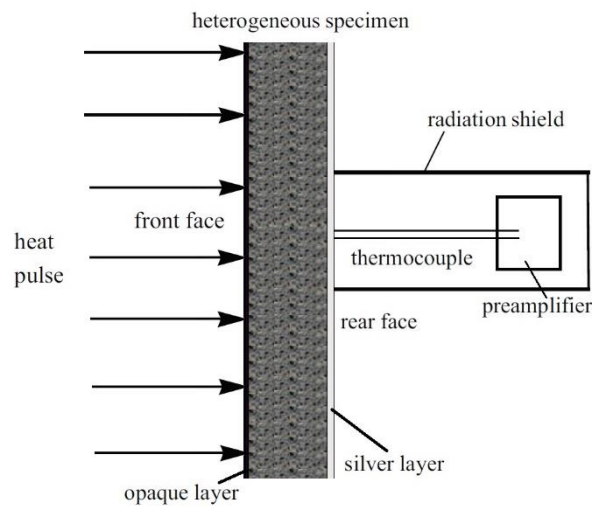


Fig. 3. Arrangement of the heat pulse experiments [15].

## EVALUATION METHOD

### Evaluation with the Fourier-Theory

The analytical solution of the Fourier equation for the rear side is [15]:

$$T(x = 1, t) = Y_0 \exp(-ht) - Y_1 \exp(x_F t), \quad x_F = -2h - \alpha\pi^2, \quad t > 30 \quad (8)$$

Which is analogous with the classical known ‘one-term solution’. First, the heat transfer coefficient  $h$  is estimated by selecting two temperature values ( $T_1$  and  $T_2$ , see Figure 4) at the decreasing part of temperature history and reading the corresponding time instants ( $t_1$  and  $t_2$ ). In this region  $\exp(x_F t) \approx 0$ ,

$$h = -\frac{\ln\left(\frac{T_2}{T_1}\right)}{t_2 - t_1}. \quad (9)$$

While  $h$  can be determined from the rear side temperature history, it should be noted that the sample is small and as long as  $h \cdot A_h$  is constant ( $A_h$  is the surface area where heat transfer

occurs), it is not necessary to determine a heat transfer coefficient for all surface. In Fourier theory, the thermal diffusivity can be expressed explicitly [8, 15], i.e.

$$\alpha_F = 1,38 \cdot \frac{L^2}{\pi^2 t_{1/2}}, \quad (10)$$

and can be determined immediately after reading  $t_{1/2}$ . The thermal diffusivity is the ratio of the thermal conductivity  $\lambda$  and the specific heat capacity  $\rho c$ . Then comes the maximum of the temperature history ( $T_{max}$ ), where the moment of time  $t_{max}$  can be read when  $T_{max}$  occurs. This gives the heat transfer coefficients, the thermal diffusivity and  $T_{max}$ , which are used in the Guyer-Krumhansl theory.

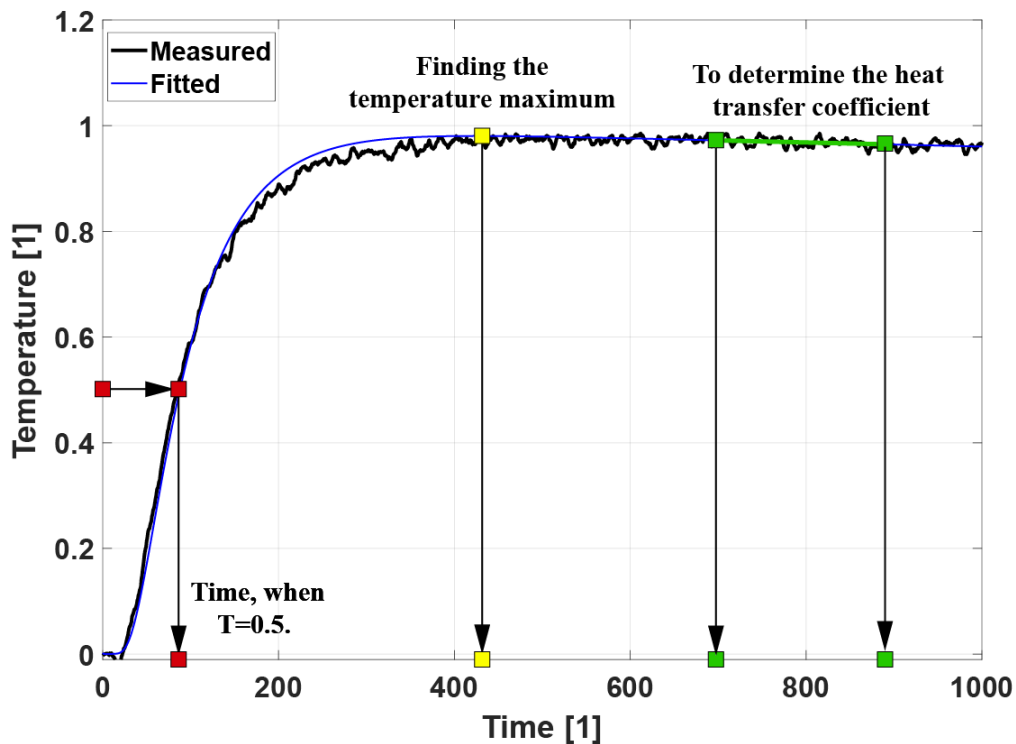


Fig. 4. Schematic representation of the Fourier evaluation method, where the dimensionless time is scaled by the heat pulse, which is 0.01 sec. The green section shows the determination of the heat transfer coefficient, the red squares show the meaning of  $t_{1/2}$  and the yellow squares show the location of the maximum temperature [8].

### Evaluation with the Guyer-Krumhansl Theory

The situation becomes more difficult in this case, because in contrast to the Fourier theory, it consists of two ‘time constants’ ( $x_1$  and  $x_2$ ) instead of one ( $x_F$  in Fourier theory). Consequently, it is not easy to find these constants. To check the effect of the simplifications made in the following, a parameter analysis was carried out for all possible  $\tau_q$  and  $\kappa^2$  values that may be possible in practice and beyond. However, beyond these, we always had to restrict ourselves to a region  $3 > \kappa^2 / (\alpha \tau_q) \geq 1$ . The lower limit expresses the Fourier case, and all other combinations fall in the over-diffusive region. The highest ratio observed in the experiments so far has been around 2.5, so a value of 3 should be appropriate. For  $\kappa^2$ , the region is  $0.02 < \kappa^2 < 1$ . We would like to emphasize that the GK theory is not restricted to this region, it also allows the under-diffusive (‘wave-like’) case, which would be most similar

to the MCV solution (Figure 2). In the GK theory, the rear side temperature history can be expressed as follows [15]

$$T(x = 1, t > 40) = Y_0 \exp(-ht) - Z_1 \exp(x_1 t) - Z_2 \exp(x_2 t), \quad x_1, x_2 < 0, \quad (11)$$

Which is also a 'one-term solution'. In the following, we present a step-by-step [8] approach to the determination of the GK parameters, which is illustrated in Figure 5.

Step 1/A. It can be observed (Figure 1) that the temperature predicted by Fourier's theory is close to the measured temperature at the beginning of the process, then rises more rapidly as it approaches the maximum. In other words, the same temperature is reached more quickly in this region with Fourier's theory (usually around 0.7-0.95). Mathematically, this can be expressed by formally writing the equations of Fourier and GK theory as follows where the fraction on the right is close to 1. It would be possible to introduce a correction factor for  $x$  in the iteration procedure if we knew more about  $\tau_q$  and  $\kappa^2$ . After rearrangement, we obtain the following closed formula for  $x_1$ :

$$x_1 = x_F \frac{t_{F1} - t_{F2}}{t_{m1} - t_{m2}}. \quad (16)$$

We take 80-90% of  $T_{max}$ , and then take the mean of the next 20 subsequent measurement points as  $x_1$ . Mathematically, closer data pairs should perform better, but this is not the case due to the uncertainty of the measurement data. In our experience, the mean offers a more consistent value for  $x_1$ .

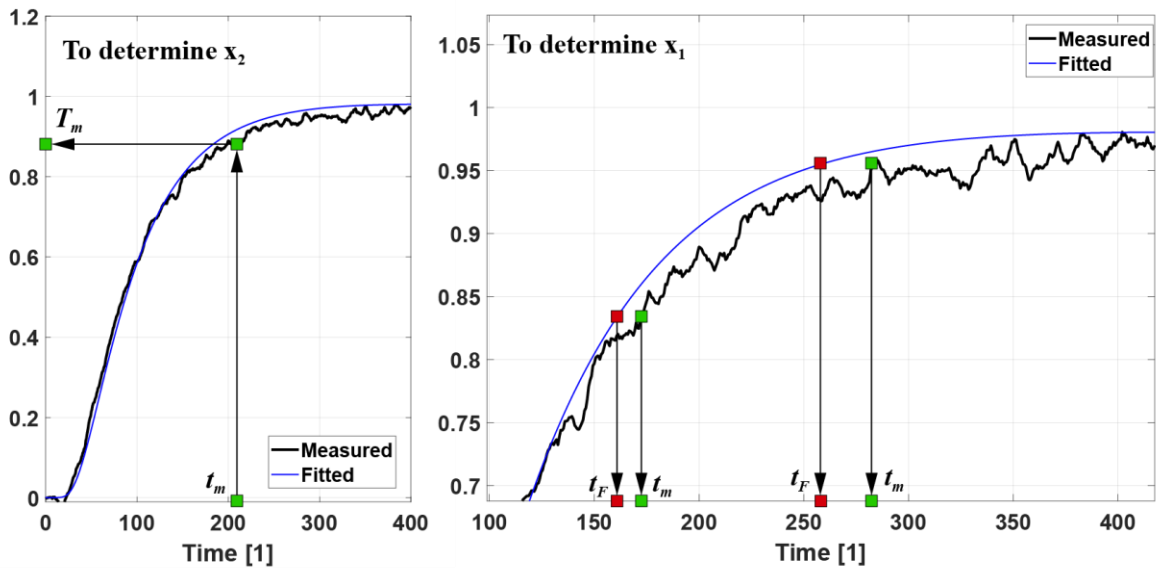


Fig. 5. The schematic representation of the evaluation method using the Guyer-Krumhansl theory. Here, the 'fitted curve' belongs to the Fourier equation [8].

- Step 1/B. In parallel with part A, we can determine the coefficient  $Z_1$  for each  $t_m$  and each corresponding  $x_{1,m}$ ,

$$Z_{1,m} = -\exp(-x_{1,m} t_m) (T_m - Y_0 \exp(-ht_m)) \quad (17)$$

where the subscript  $m$  represents the value for a measurement point. After 20 subsequent measurement points, the average value of the set  $\{Z\}_{1,m}$  is taken.

- Step 2. In this step, to obtain  $x_2$  we rearranged the following equation
 
$$T = Y_0 \exp(-ht) - Z_1 \exp(x_1 t) - Z_2 \exp(x_2 t), \quad (18)$$

to  $x_2$  and calculate the average of the values for each  $t_m$  giving the average value of the set  $\{x_{2,m}\}$ . Unfortunately, for noisy data, this approach can result in positive  $x_2$  values. These values must be excluded, otherwise they may lead to instability and meaningless results. Careful filtering of the data can help to solve this problem and in fact we use this to facilitate the calculation.

- Step 3. Now that we have both exponents and coefficients, the analytical expressions can be explicitly rearrange to the GK parameters and the  $\alpha_{GK}$ ,  $\tau_q$  and  $\kappa^2$  values can be calculated [8].
- Step 4. Each parameter of the temperature history can be characterized with  $R^2$ , the coefficient of determination [8].

In practice, this evaluation method reduces the number of 'fitted' parameters. Moreover, it is limited to a relatively narrow range, i.e. the evaluation procedure takes only a few seconds instead of running computationally expensive algorithms that take hours.

## NON-FOURIER THERMAL BEHAVIOUR

The evaluation procedure described above [8] is used on several rock samples, the results of which are shown below. It is noted that the samples are manufactured by Kómerő Ltd. as the necessary infrastructure and technology is available there. The thin 1.9 mm thick rock sample is challenging to produce due to, for example, its fragility, so only one of each thickness of rock is available.



Fig.6. Szarsomlyo Limestone Formation sample (left) and Szaszvar Limestone Formation sample (right).

## SZARSOMLYO LIMESTONE FORMATION

The results obtained from the evaluation for the Szársomlyó limestone formation are shown in Table 1. The non-Fourier effect is observed for the thinner samples. As the thickness increases, the Fourier theory fits the temperature history well. The evaluations are shown in Figures 7-9. Notably, the difference in thermal diffusivities for both models are significant between cases of 2 mm and 2.15 mm thicknesses. For thicker samples, the Fourier model becomes adequate.

Table 1. Summary of fitted thermal parameters of the Szársomlyó limestone formation.

Szársomlyó limestone formation	$\alpha_F$	$\alpha_{GK}$	$\tau_q$	$\kappa^2$
	$10^{-6}[m^2/s]$	$10^{-6}[m^2/s]$	[s]	$10^{-7}[m^2]$
2 mm	0.5113	0.5812	0.4180	0.0835
2.15 mm	1.1186	1.0254	0.4010	0.1127
2.85 mm	1.1413	-	-	-
3.85 mm	1.1197	-	-	-

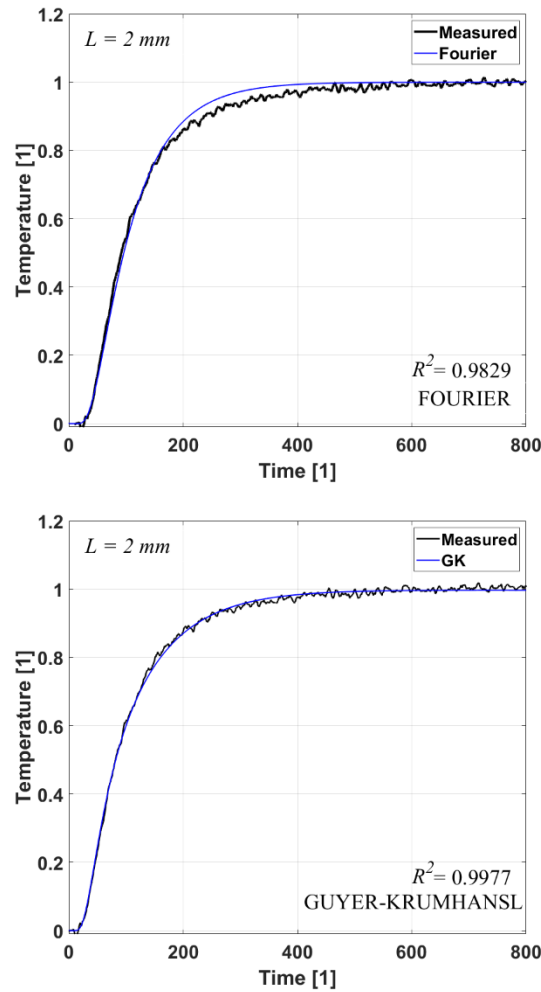


Fig. 7. Rearside temperature history in the L = 2 mm sample of the Szársomlyó limestone formation.



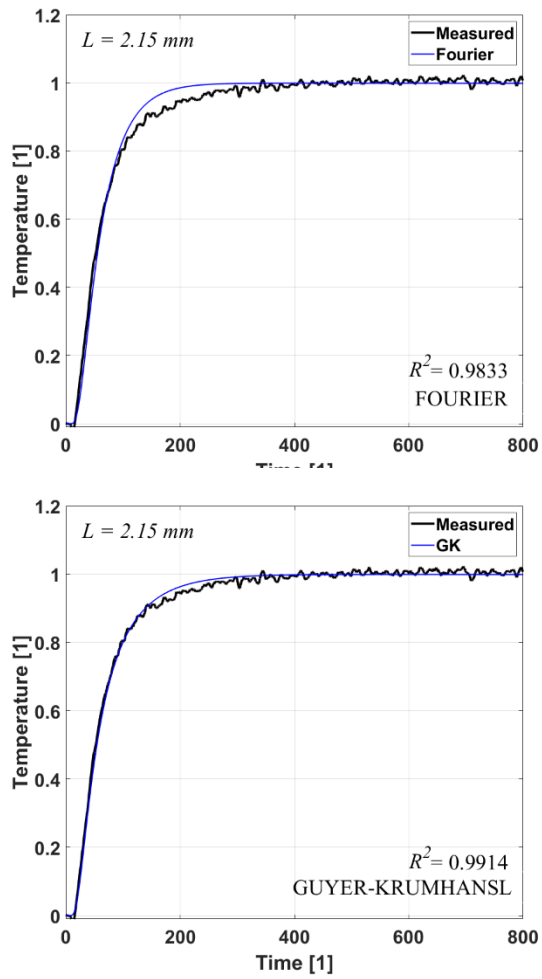


Fig. 8. Rearside temperature history in the  $L = 2.15$  mm sample of the Szársomlyó limestone formation.

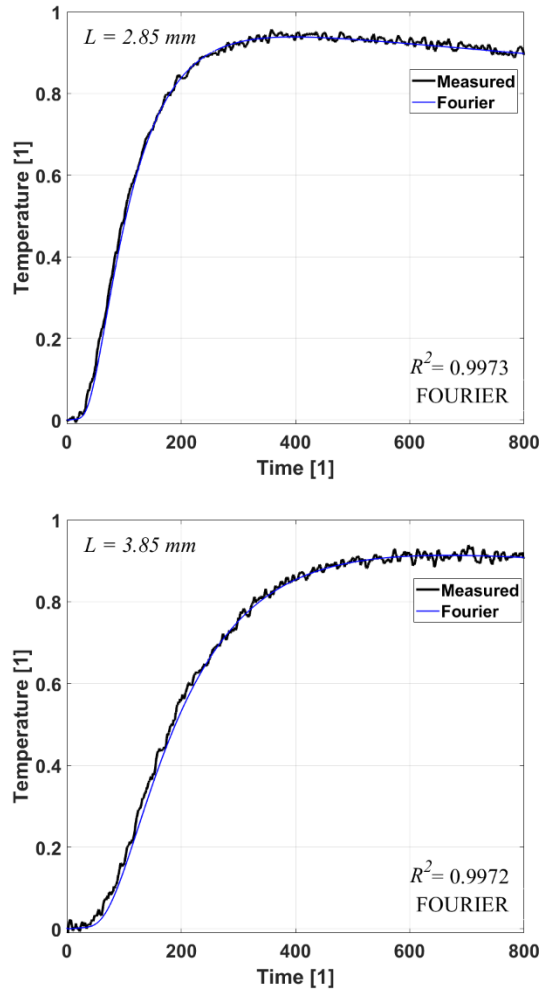


Fig. 9. Rearside temperature history in the  $L = 2.85 \text{ mm}$  and  $L = 3.85 \text{ mm}$  samples of the Szársomlyó limestone formation.

### Szászvár Limestone Formation

In the case of the Szászvár Limestone Formation, the results of the evaluation are shown in Table 2.

Table 2. Summary of fitted thermal parameters of the Szászvár limestone formation

Szászvár limestone formation	$\alpha_F$	$\alpha_{GK}$	$\tau_q$	$\kappa^2$
	$10^{-6}[\text{m}^2/\text{s}]$	$10^{-6}[\text{m}^2/\text{s}]$	[s]	$10^{-7}[\text{m}^2]$
3.05 mm	1.4048	1.4505	0.4273	0.0815
3.8 mm	0.8598	0.8815	0.5229	0.0409
3.9 mm	1.251	-	-	-

In the case of the rocks, a similar phenomenon can be observed as in the case of the Szársomlyó sample. On thinner samples, a non-Fourier effect is observed, which disappears with increasing sample thickness and the Fourier equation models our rock sample well.

## SUMMARY AND DISCUSSION

We have developed an algorithm to efficiently evaluate room temperature heat pulse experiments in which a non-Fourier effect could present. This is called over-diffusive propagation and detunes the thermal diffusivity, even when the deviation is seemingly small or negligible for the rear side temperature history. The presented method is based on the analytical solution of the Guyer-Krumhansl equation, including temperature-dependent convection boundary condition, thus the heat transfer to the environment can be immediately included in the analysis.

We observed the size dependence of the thermal diffusivity for both heat conduction models, therefore it is not unique for the non-Fourier behaviour but also could forecast the presence of over-diffusion. That effect originates in the heterogeneities. Due to the equipment limitations, it is not possible to use samples with representative size, i.e., a size for which the thermal parameters are constant by having the heterogeneous effects averaged. Unfortunately, it is difficult to produce such thin rock samples, therefore it limits the measurements capabilities, however, these results stand as a strong motivation to continue the research and discover these effects more deeply. That dependence is strong for both rock types. Interestingly, the increase could be significant, more than 50 %. Additional size effect can be observed for the over-diffusion phenomenon, too. The modelling capabilities of the Fourier equation are better for thicker samples. Overall, it motivates further research and the need for more samples, providing a better resolution in thickness. Moreover, we also need multiple samples from the same thickness in order to investigate the sudden changes in the size dependence of thermal diffusivity.

We believe that this procedure lays the foundations for more practical engineering applications of non-Fourier models, especially for the best candidate among all of them, the Guyer-Krumhansl equation. It sheds new light on the classical and well-known flash experiments, and we provide the necessary tools to find additional thermal parameters to achieve a better description of heterogeneous materials. It becomes increasingly important with the spreading of composites and foams and helps characterize 3D printed samples with inclusions. With continuing the experiments, our goal is to find a relationship between the non-Fourier coefficients and the material structure. For instance, we aim to analyse multiple foam samples with different inclusion sizes, expectedly connecting production parameters to the non-Fourier effects.

## REFERENCES

1. BOTH, S.; CZÉL, B.; FÜLÖP, T.; GRÓF, Gy.; GYENIS, Á.; KOVÁCS, R.; VÁN, P. and VERHÁS J. Deviation from the Fourier law in room-temperature heat pulse experiments. *Journal of Non-Equilibrium Thermodynamics*, 2016, Vol. 41.
2. VÁN, P.; BEREZOVSKY, A.; FÜLÖP, T.; GRÓF, Gy. KOVÁCS, R.; LOVAS, Á. and VERHÁS, J. Guyer-Krumhansl-type heat conduction at room temperature. *EPL*, 2017, Vol. I118, No. 10005.
3. PARKER, W. J.; JENKINS, R. J.; BUTLER, C. P.; and ABBOTT, G. L. Flash method of determining thermal diffusivity, heat capacity, and thermal conductivity. *Journal of Applied Physics*, 1996, Vol. 32, No. 9, P.1679–1684.

4. FEHÉR, A.; MARKOVICS, D.; FODOR, T.; KOVÁCS, R. Size effects and non-Fourier thermal behaviour in rocks. *ISRM International Symposium – EUROCK 2020*, 14-19 June, physical event not held, 2020.
5. JAMES, H. M. Some extensions of the flash method of measuring thermal diffusivity. *Journal of Applied Physics*, 1980, Vol. 51, No.9, P.4666-4684
6. FÜLÖP, T.; KOVÁCS, R.; LOVAS, Á. RIETH, Á. FODOR, T.; SZÜCS, M.; VÁN, P. and GRÓF, Gy. Emergence of non-Fourier hierarchies. *Entropy*, 2018, Vol. 20, No. 11, P. 832.
7. RIETH, Á. KOVÁCS, R. and FÜLÖP, T. Implicit numerical schemes for generalized heat conduction equations. *International Journal of Heat and Mass Transfer*, 2018, Vol. 126, P. 1177-1182.
8. FEHÉR, A.; KOVÁCS, R. On the evaluation of non-Fourier effects in heat pulse experiments. *International Journal of Engineering Science*, 2021, Vol. 169, 2021, No. 103577, ISSN 0020-7225.
9. VÁN, P. Theories and heat pulse experiments of non-Fourier heat conduction. *Communications in Applied and Industrial Mathematics*, 2016, Vol.7, P. 150-166.
10. MÜLLER, I.; RUGGERI, T. Rational extended Thermodynamics. Springer, 1998.
11. CIMMELI, V. A. Different thermodynamic theories and different heat conduction laws. *Journal of Non-Equilibrium Thermodynamics*, 2009, Vol. 34, P. 299-333.
12. JOSEPH, D. D.; PREZIOSI, L. Heat waves. *Reviews of Modern Physics*, 1989, Vol. 61.
13. SOBOLEV, S. L. Local non-equilibrium transport models. *Physics-Uspokhi*, 1997, Vol. 40, P. 1043-1053.
14. SOBOLEV, S. L. Nonlocal diffusion models: Application to rapid solidification of binary mixtures. *International Journal of Heat and Mass Transfer*, 2014, Vol, 71, P. 295-302.
15. FEHÉR, A.; LUKÁCS, N.; SOMLAI, L.; FODOR, T.; SZÜCS, M.; FÜLÖP, T.; VÁN, P.; KOVÁCS, R. Size effects and beyond-Fourier heat conduction in room-temperature experiments. *Journal of Non-Equilibrium Thermodynamics*, 2021, Vol. 46, No. 4, P. 403-411.
16. FÜLÖP, T.; KOVÁCS, R.; and VÁN, P. Thermodynamic hierarchies of evolution equations. *Proceedings of the Estonian Academy of Sciences*, 2015, Vol. 64, P. 389-395.